Journal of Magnetic Resonance 204 (2010) 124–130

Contents lists available at ScienceDirect

Journal of Magnetic Resonance

journal homepage: www.elsevier.com/locate/jmr

# Quantitative $^{13}C$ NMR spectroscopy using refocused constant-time INEPT, Q-INEPT-CT

A.V. Mäkelä *, I. Kilpeläinen, S. Heikkinen

*Laboratory of Organic Chemistry, Department of Chemistry, University of Helsinki, P.O. Box 55, FI-00014 University of Helsinki, Finland*

ARTICLE INFO

*Article history:*
Received 19 August 2009
Revised 29 January 2010
Available online 23 February 2010

*Keywords:*
Quantitative NMR
$^{13}C$ NMR
Q-INEPT-CT
Q-DEPT

ABSTRACT

Quantitative NMR spectroscopy is a useful tool for the analysis of various mixtures. Usually $^{1}H$ NMR is used for quantitative measurements, but in many cases the better signal dispersion offered by $^{13}C$ NMR is beneficial. However, the low natural abundance of $^{13}C$ and long $T_1$ relaxation times make the acquisition of quantitative $^{13}C$ spectra with adequate signal-to-noise ratio time-consuming. The use of polarization transfer experiments such as DEPT or INEPT can offer improved signal intensity and faster repetition rate, but yield non-quantitative results. In this paper we present a pulse sequence based on constant-time INEPT, Q-INEPT-CT, which is capable of producing quantitative carbon spectra with better sensitivity and/or in less time than traditional quantitative $^{13}C$. Additionally, the constant length of the sequence means that signal loss due to relaxation effects can be relatively easily corrected. Thus, the presented sequence is a valuable tool when quantitative carbon data is required quickly and/or low-concentration samples are involved.



## 1. Introduction

While quantitative $^{1}H$ NMR spectra are simple to obtain, the relatively small $^{1}H$ spectral range easily leads to severe overlap when complex mixtures or large molecules are analyzed. In some cases, techniques such as signal deconvolution and various statistical methods can be used to extract information even when signal overlap seems to obscure all meaningful information [1]. $^{13}C$ NMR spectroscopy offers a much improved signal dispersion and hence superior resolving capacity. However, the low natural abundance of $^{13}C$ nuclei, smaller gyromagnetic ratio and long $T_1$ relaxation times lead usually to very long measurement times.

If increasing the sensitivity of the NMR instrument itself is not considered, increasing carbon signal intensity can only be accomplished by increasing carbon polarization or by increasing longitudinal relaxation rate and thus allowing more accumulations of the magnetization in the same amount of time. The latter can be achieved via relaxation reagents, but significant signal broadening and other problems will usually occur. Furthermore, this is typically not an option if the sample has to be recovered. The carbon polarization itself can be affected by NOE transfer from protons, cross polarization, or utilizing polarization transfer by RF-pulses/delays, i.e. via INEPT [2] or DEPT [3]. Unfortunately, all of these techniques produce different enhancement factors depending on the molecular structure and other variables, rendering them unsuitable for quantitative use as such.

Any technique used for quantitative spectroscopy should provide equal enhancement for every carbon. From the aforementioned techniques, NOE is strongly dependent on various factors, such as number of proximate protons, mobility of the molecule and relaxation. Cross polarization is also difficult to control, and requires careful matching of RF-field strengths to work. These reasons render NOE and cross polarization practically unsuitable for quantitative use. On the other hand, polarization transfer via RF-pulses and delays (i.e. INEPT, DEPT) depends only on the heteronuclear coupling constant, $^{1}J_{CH}$, and on the number of protons attached to the carbon. While the $^{1}J_{CH}$ coupling constants depend on the molecular structure, they vary within a relatively small range, and for most structures $^{1}J_{CH}$ values are between 115 and 170 Hz.

All experiments employing polarization transfer via heteronuclear coupling depend on the correct evolution of the *J*-coupling between proton and carbon during the pulse sequence. A single polarization transfer step can only be optimally tuned for one particular heteronuclear coupling constant value, and any deviation from this optimal value will result in reduced polarization transfer efficiency. The length of refocusing period (in INEPT) or editing pulse (in DEPT) will also produce different responses depending on the number of protons attached. While it is clear from the above discussion that a single polarization transfer step always results in non-uniform enhancements when multiple *J*-coupling constant values are involved, a combination of differently optimized steps

* Corresponding author.
*E-mail address:* valtteri.makela@iki.fi (A.V. Mäkelä).

1090-7807/$ - see front matter © 2010 Elsevier Inc. All rights reserved.
doi:10.1016/j.jmr.2010.02.015

can complement each other and yield more uniform response. This idea has been exploited in a previously reported Q-DEPT sequence [4] and its recently revised version Q-DEPT+ [5], while the technique was originally used to obtain quantitative 2D $^{1}H$–$^{13}C$ spectra, Q-HSQC [6,7]. In these methods, a set of optimized delays and/or edit pulses are cycled resulting in a near-uniform response for a broad range of *J*-couplings, making quantitative results possible. While Q-DEPT can be used to obtain quantitative carbon spectra, it uses variable length pulses, which are sensitive to RF-inhomogeneity and calibration errors. Also, the pulse sequence duration itself varies significantly depending on modulation (4–21 ms) [5], making it unfavorable for fast relaxing species. Another approach, presented here, is the use of INEPT sequence as the basis of the polarization transfer, which avoids these limitations.

## 2. Theory

The refocused INEPT sequence can be modulated in a similar way as DEPT to obtain quantitative data (Q-DEPT [4,5]). Like DEPT, refocused INEPT can be modulated with two parameters affecting the intensity and phase of the resulting carbon signals. The main difference, from the modulation point of view, is that the variable length editing pulse of DEPT is substituted by the variable length refocusing period in INEPT. DEPT also relies on the creation of multiple quantum magnetization, while INEPT does not, and thus the interdependency between evolution delays and the observed magnetization is simpler in INEPT. In addition, as the edition/modulation is based on delay duration rather than pulse lengths, the effect of RF-inhomogeneity is less pronounced.

The magnetization resulting from the refocused INEPT experiment depends on the lengths of the INEPT ($\Delta_1$) and refocusing ($\Delta_2$) periods, along with the coupling constant $^{1}J_{CH}$ between the carbon and the proton(s) in question. The equations describing the signal intensity for CH, $CH_2$ and $CH_3$ groups in refocused INEPT can be derived with product operator formalism [8–10]:

$$I_{CH} = \sin(\pi J_{CH}\Delta_1) * \sin(\pi J_{CH}\Delta_2) \quad (1)$$

$$I_{CH_2} = \sin(\pi J_{CH}\Delta_1) * 2\sin(\pi J_{CH}\Delta_2)\cos(\pi J_{CH}\Delta_2) \quad (2)$$

$$I_{CH_3} = \sin(\pi J_{CH}\Delta_1) * 3\sin(\pi J_{CH}\Delta_2)\cos^2(\pi J_{CH}\Delta_2) \quad (3)$$

where $I_{CH}$, $I_{CH2}$ and $I_{CH3}$ represent magnetization for different carbon multiplicities, $J_{CH}$ is the prevailing coupling constant, $\Delta_1$ and $\Delta_2$ are the lengths of the INEPT and refocusing periods, respectively.

Using Eqs. (1)–(3), the theoretical response of refocused INEPT experiment utilizing any combination of $\Delta_1$ and $\Delta_2$ modulations can be calculated, and thus optimal combination of modulations with nearly uniform response over suitable $^{1}J_{CH}$ range can be derived. Here, Eqs. (1)–(3) were implemented in a simple computer program using the C programming language, which was then used to test all combinations possible with specified range of $\Delta_1$ and $\Delta_2$ values, determining the one with most uniform response. Various modulation schemes were considered, but after initial calculations, simultaneous modulation of both periods using eight pairs total was chosen. As the amount of potential combinations increases vastly with every additional $\Delta_1$ and $\Delta_2$ value introduced, only a limited quantity of values could be tested within reasonable time with the program. These coarsely optimized modulations were optimized further by a GRG quasi-Newton non-linear regression algorithm implemented in the Microsoft Excel solver routine [11].

For additional optimization of the sequence for quantitative use, two notable improvements were made. First, as refocused INEPT has two carbon 180° pulses, the offset effects can easily become a problem, at least when considering quantitative use. To improve offset performance, both pulses were replaced with six-element composite pulses developed by Shaka et al. [12,13], offering good inversion/refocusing properties over large bandwidth (Fig. 3). The 180° pulses were sandwiched between gradient pulses, purging any magnetization not experiencing 180° inversion. Secondly, a constant-time version of the sequence was developed (Fig. 1). This approach is beneficial, because with constant length any relaxation effects will be of the same magnitude, regardless of the modulation used. In addition, homonuclear $J_{HH}$-evolution is constant, thus allowing for an easy application of intensity correction factor if desired.

The constant-time feature is implemented by shifting the carbon 180° pulse (in the INEPT period) and proton 180° pulse (in the refocusing period) earlier to affect the total evolution experienced. As the evolution of $^{1}J_{CH}$ progresses to the reverse direction after the first 180° pulse, the shifting can be used to reduce the total amount of evolution experienced. For example, in the INEPT period, the proton 180° pulse must be centered to refocus chemical shift evolution, and thus the delays in both sides of the pulse must be equally long (Fig. 1):

$$\Delta_{1A} + \Delta_{1B} = \Delta_{1C} \quad (4)$$

If the carbon pulse is shifted earlier, the total $^{1}J_{CH}$ evolution ($\Delta_1$) is:

$$\Delta_1 = \Delta_{1A} - \Delta_{1B} + \Delta_{1C} \quad (5)$$

Eq. (5) simplifies further by substituting $\Delta_{1C}$ from Eq. (4):

$$\Delta_1 = 2 * \Delta_{1A} \quad (6)$$

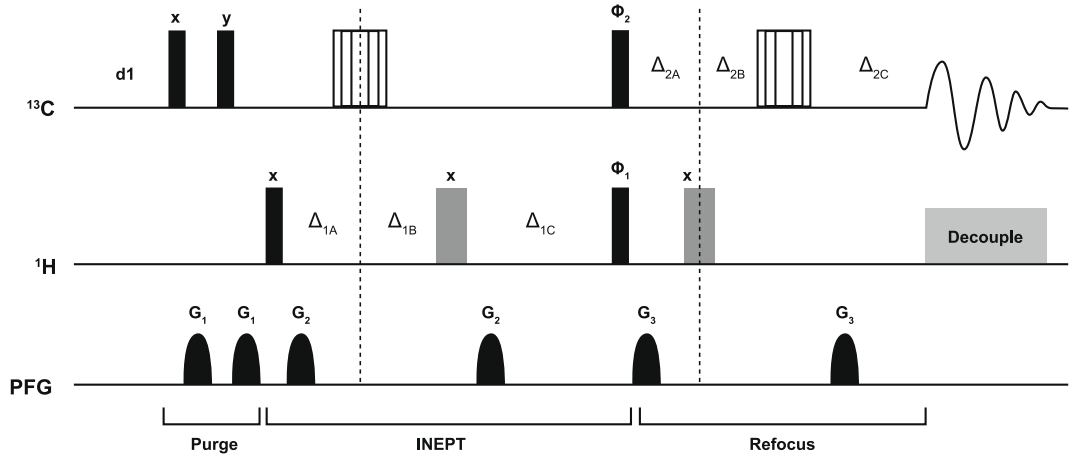


**Fig. 1.** Q-INEPT-CT-pulse sequence. Narrow black and wide gray bars represent 90° and 180° pulses, respectively. The 180° composite pulses are marked by multiple narrow white bars. Phases are cycled as follows: $\phi_1 = y, -y$ $\phi_2 = x, x, -x, -x$ $\phi_{rec} = x, -x, -x, x$.

**Table 1**
The original and time-restricted modulations of Q-INEPT-CT, optimized for $^1J_{CH}$-couplings between 115–170 Hz. The last row (Min–max difference) presents the difference between minimum and maximum signal intensity, in percents of the maximum signal. The theoretical response curve is presented in Fig. 2

| Modulation # | Original mod. | | Time rest. mod. | |
|---|---|---|---|---|
| | $\Delta_1$ (ms) | $\Delta_2$ (ms) | $\Delta_1$ (ms) | $\Delta_2$ (ms) |
| 1 | 2.9845 | 3.5865 | 5.0000 | 3.4146 |
| 2 | 2.1038 | 1.2160 | 5.0000 | 3.4146 |
| 3 | 2.1591 | 1.1601 | 2.2748 | 1.8994 |
| 4 | 5.0870 | 3.7347 | 2.0373 | 1.5505 |
| 5 | 2.4326 | 2.8578 | 1.5143 | 1.5079 |
| 6 | 1.9198 | 1.1739 | 1.0079 | 1.5113 |
| 7 | 2.1328 | 1.1341 | 1.0000 | 1.7575 |
| 8 | 8.8292 | 4.3309 | 1.0000 | 1.4250 |
| Min–max difference | 3.64 % | | 12.73 % | |

The total $^1J_{CH}$ evolution is thus $2*\Delta_{1A}$ and the maximum possible evolution time is achieved when $\Delta_{1A} = \Delta_{1C}$ (and $\Delta_{1B} = 0$), rendering it effectively to a regular INEPT period. Therefore, in the constant-time sequence, the length of the evolution period must be at least as long as the longest desired evolution time. This can be achieved by choosing delay $\Delta_{1MAX}$, which is equal or longer than the longest evolution time needed, and calculating the delays with following equations:

$$\Delta_{1A} = \frac{\Delta_1}{2} \tag{7}$$

$$\Delta_{1B} = \frac{\Delta_{1MAX}}{2} - \Delta_{1A} \tag{8}$$

$$\Delta_{1C} = \frac{\Delta_{1MAX}}{2} \tag{9}$$

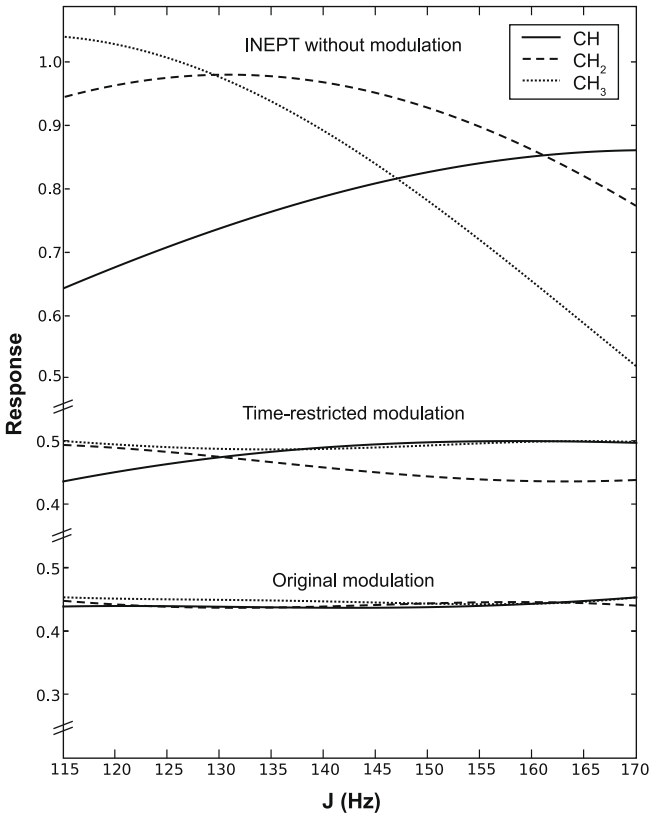


**Fig. 2.** Calculated response of INEPT and Q-INEPT-CT experiments for $^1J_{CH}$-couplings from 115–170 Hz. The INEPT experiment (top) was optimized for 145 Hz, with a commonly used refocusing delay of $0.3/^1J_{CH}$ to provide positive signals for all carbon types. For Q-INEPT-CT experiments, the modulations from Table 1 were used.

In the actual pulse sequence implementation, $\Delta_{1MAX}$ is chosen to be slightly longer than the maximum evolution time needed. It can be also noted that with some instruments, the composite carbon pulse in the INEPT period can be quite long, as it is about ~5.5 times longer than a hard rectangular 180° pulse. This is not a problem however, as the carbon magnetization remains in the *z*-axis and $^1J_{CH}$ evolution will be active during the pulse [14].

Finally, a short 4-step phase cycle was implemented (see Fig. 1 for details) to allow for a reasonable minimum amount of transients. The modulation scheme necessitates 8 transients to complete, which translates in to minimum of 32 transients for a full cycle. To aid the phase cycle to select only magnetization originating from protons, a gradient block was added to the beginning of the sequence to purge all natural $^{13}$C-magnetization.

## 3. Results and discussion

The pulse sequence (Fig. 1) was initially evaluated by measuring quantitative spectra from a model compound mixture containing ethylbenzene and cholesterol (sample #1). Additionally, the actual responses from different modulations were measured by varying the $\Delta_1$ and $\Delta_2$ delays separately from 1.0 to 10.8 ms in 0.2 ms steps, using concentrated ethylbenzene sample. Unfortunately, the sequence failed to perform as well as the theoretical calculations suggest, yielding worse data than traditional quantitative carbon measurements. However, it was noted from the modulation-response measurements that while the responses agreed well with the theoretical calculations at smaller values, they started to deviate with longer evolution times (~5 ms). Therefore, an alternative optimization was created with restricting maximum evolution time to 1.0–5.0 ms for both $\Delta_1$ and $\Delta_2$ (Table 1).

The calculated responses for both modulations and a regular INEPT are presented in Fig. 2. As seen in Fig. 2, the time-restricted modulation has less uniform polarization transfer profile com-

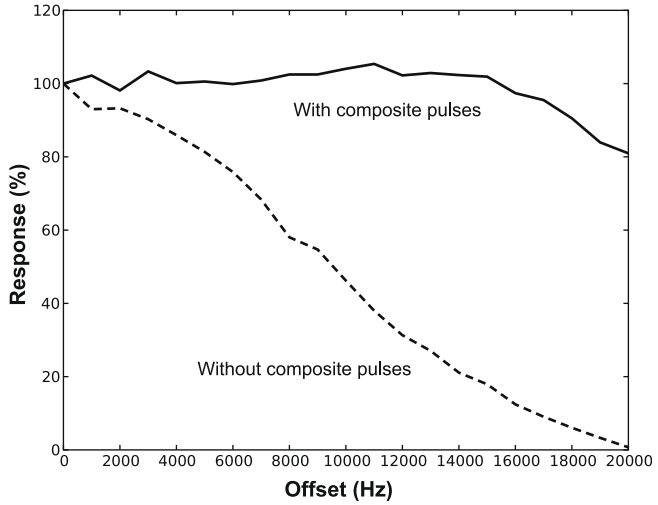


**Fig. 3.** The offset performance of Q-INEPT-CT with and without carbon composite inversion pulses. The signal of carbon #3 was measured from 21 spectra, which were acquired by offsetting the transmitter in 1000 Hz steps, starting from on-resonance. Using normal 180° pulses, the response drops by almost 20% at a 5 kHz offset (~33 ppm with 600 MHz spectrometer), while with composite pulses the response remains within ~5% for 17 kHz yielding maximum usable spectral window of 34 kHz (~227 ppm with 600 MHz spectrometer). The time-restricted modulation scheme was used for Q-INEPT-CT. Relaxation delay was 18 s and the acquisition time was 2 s. Spectrum width was 50 kHz. $^{13}$C and $^1$H pulses were applied at 17.5 and 46.3 kHz RF-field strengths, respectively (corresponding to 14.25 and 5.4 μs 90° pulses). Integration was carried out from absolute value spectra. All the other parameters were the same as those described in the experimental section.

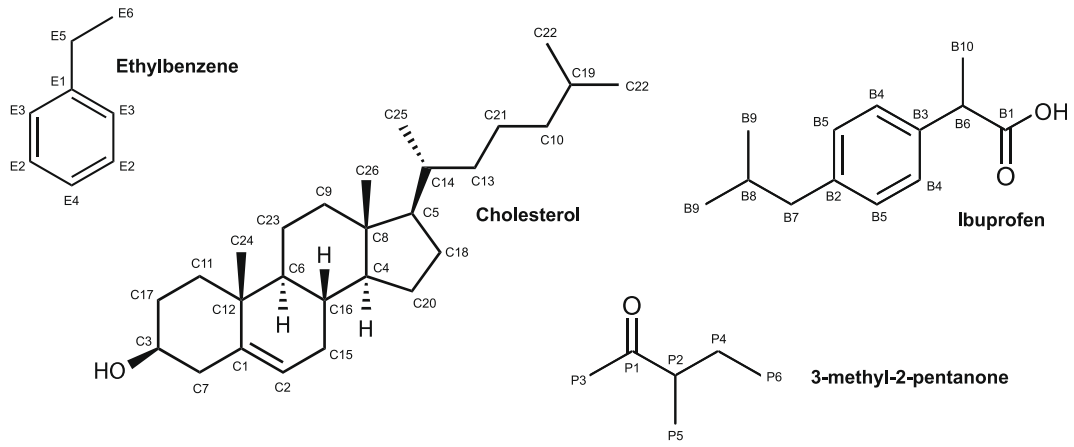


**Fig. 4.** Carbon assignments for the molecules used in evaluation samples.

pared to the original modulation. Maximum expected transfer from the modulated sequences is about 0.45–0.50, which translates to signal gain of a factor of two ($\sim 0.5 * \gamma_H/\gamma_C$). This can be compared to regular INEPT, with efficiencies varying from slightly over 0.5 to 1.05 translating to a 2.0–4.2 gain in intensity ($CH_3$-groups) in the same $^1J_{CH}$ range. The modulation scheme thus loses on average about 50% of signal compared to the theoretical maximum for any carbon, in exchange for the more uniform transfer across different couplings and carbon types. However, the theoretical maximum is rarely achieved as the optimization of traditional INEPT is always a compromise. For example, in Fig. 2, transfer efficiencies less than 0.8 are achieved for both CH and $CH_3$ carbons, with low and high $^1J_{CH}$, respectively.

The derived modulations were evaluated using the ethylbenzene/cholesterol sample (sample #1). For both modulations, four spectra with identical parameters were measured. For comparison, four traditional quantitative $^{13}C$ spectra were also acquired (Figs. 5 and 6). The same exact regions were integrated from every spectra and resulting integrals were averaged between the four identical measurements to minimize errors arising from measurement or processing of a single spectrum. The integral values were then divided by the number of carbons responsible for the signal, and normalized by dividing the signals with the average amount of signal obtained per carbon. The results are presented in Tables 2 and 3 with the corresponding carbon assignments presented on Fig. 4. While the time-restricted modulation has significantly less uniform calculated response (Fig. 2), the experimental data shows significantly improved results compared to the original modulation. The original modulation produced excellent results with the small molecule, ethyl benzene, but the results for cholesterol are much worse.

As the time-restricted version of the pulse sequence seemed to work adequately, the sequence was further evaluated with another sample containing roughly 1:1 concentration of ibuprofen and 3-methyl-2-pentanone (sample #2). Four Q-INEPT-CT spectra with both modulations were acquired and for comparison, single quantitative carbon spectrum was recorded (Fig. 7). The spectra were processed and analyzed in the same way as with sample #1, and

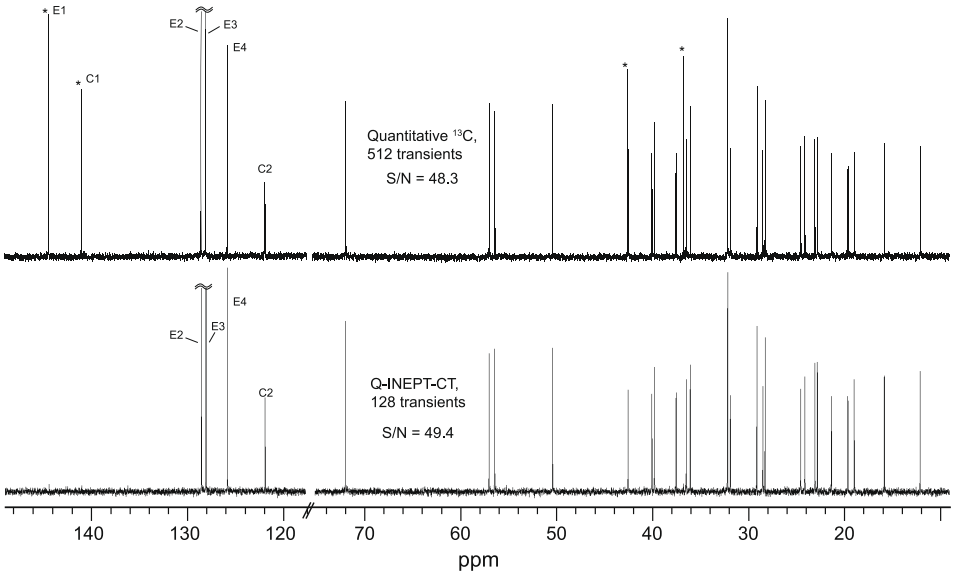


**Fig. 5.** A quantitative $^{13}C$ spectrum compared to Q-INEPT-CT spectrum, obtained from the sample #1 (ethylbenzene and cholesterol). Quaternary carbon signals are marked by an asterisk in the quantitative $^{13}C$ spectrum. The $^{13}C$ experiment, employing a 45° excitation pulse, needs about four times as many transients to achieve similar signal-to-noise ratio with the Q-INEPT-CT experiment. The upfield portion of the spectra is shown in detail and with labels in Fig. 6. Signal-to-noise values are presented in the figure (signal at ~72 ppm, noise 65–70 ppm). Acquisition parameters are presented in the experimental section. The total measurement times were 14 h 14 min and 3 h 39 min for the quantitative $^{13}C$ and Q-INEPT-CT spectra, respectively.

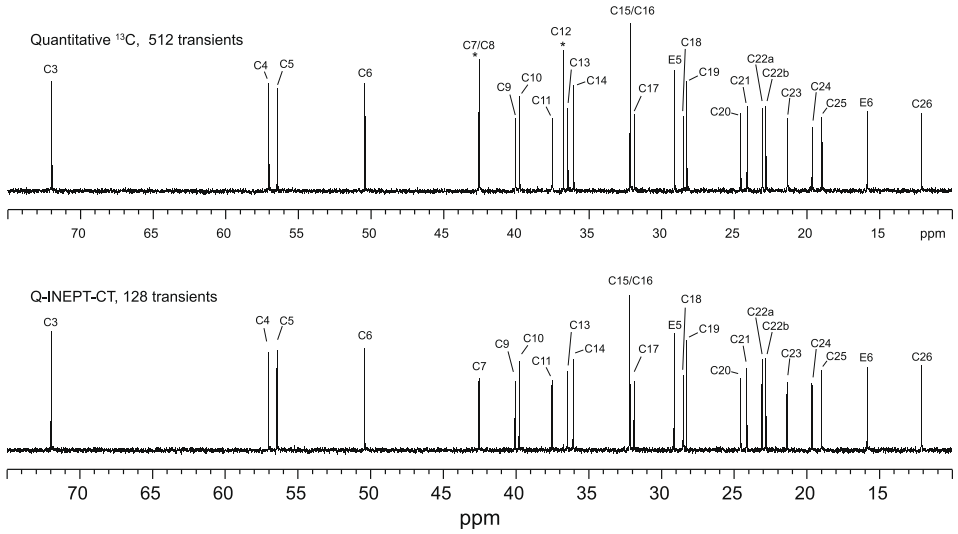


**Fig. 6.** A quantitative $^{13}C$ spectrum compared to Q-INEPT-CT spectrum, showing the signal-rich upfield portion of the spectrum, obtained from the sample #1 (ethylbenzene and cholesterol). Quaternary carbon signals are marked by an asterisk in the quantitative $^{13}C$ spectrum (note that at ~42.5 ppm, the signals of quaternary carbon C8 and protonated carbon C7 overlap).

**Table 2**
The results for ethylbenzene with both modulations and quantitative $^{13}C$. Quaternary carbon (E1) is not listed. The carbon assignments are given in Fig. 4.

| Carbon # | Chemical shift | $^{13}C$ | Q-INEPT-CT | |
|---|---|---|---|---|
| | | | Original mod. | Time rest. mod. |
| E2 | 128.52 | 1.05 | 0.97 | 0.98 |
| E3 | 128.06 | 1.04 | 1.01 | 1.04 |
| E4 | 125.80 | 1.01 | 1.00 | 1.03 |
| E5 | 29.12 | 0.95 | 1.02 | 0.99 |
| E6 | 15.84 | 0.87 | 1.03 | 0.94 |
| | Min. integral | 0.872 | 0.968 | 0.944 |
| | Max. integral | 1.047 | 1.026 | 1.038 |
| | Difference | 0.175 | 0.059 | 0.093 |
| | Difference (%) | 17.5 | 5.9 | 9.3 |

**Table 3**
The results for cholesterol with both modulations and quantitative $^{13}C$. Quaternary carbons C1, C8 and C12 are not listed. Additionally, due to heavy overlap of carbon C8 with carbon C7, it is omitted from $^{13}C$ results. The carbon assignments are given in Fig. 4.

| Carbon # | Chemical shift | $^{13}C$ | Q-INEPT-CT | |
|---|---|---|---|---|
| | | | Original mod. | Time rest. mod. |
| C2 | 121.91 | 1.13 | 1.19 | 1.17 |
| C3 | 71.99 | 1.02 | 0.98 | 1.07 |
| C4 | 57.02 | 1.04 | 1.01 | 0.95 |
| C5 | 56.44 | 1.00 | 0.91 | 0.98 |
| C6 | 50.40 | 1.01 | 1.08 | 0.97 |
| C7 | 42.53 | – | 1.12 | 1.08 |
| C9 | 40.05 | 0.97 | 1.04 | 0.99 |
| C10 | 39.78 | 1.06 | 0.97 | 1.03 |
| C11 | 37.52 | 0.96 | 1.03 | 0.99 |
| C13 | 36.46 | 0.95 | 0.94 | 0.93 |
| C14 | 36.05 | 1.03 | 0.95 | 0.92 |
| C15 & C16 | 32.16 | 1.04 | 0.98 | 0.99 |
| C17 | 31.87 | 1.02 | 0.88 | 0.99 |
| C18 | 28.49 | 1.01 | 0.82 | 0.99 |
| C19 | 28.26 | 1.04 | 0.93 | 1.02 |
| C20 | 24.55 | 0.94 | 0.85 | 0.93 |
| C21 | 24.11 | 1.00 | 0.84 | 0.95 |
| C22a | 23.07 | 0.95 | 1.13 | 1.07 |
| C22b | 22.81 | 0.98 | 1.10 | 1.03 |
| C23 | 21.35 | 0.97 | 0.95 | 0.98 |
| C24 | 19.64 | 0.94 | 1.10 | 1.04 |
| C25 | 18.98 | 0.98 | 1.15 | 1.01 |
| C26 | 12.11 | 0.90 | 1.07 | 0.92 |
| | Min. integral | 0.904 | 0.820 | 0.918 |
| | Max. integral | 1.135 | 1.187 | 1.166 |
| | Difference | 0.231 | 0.367 | 0.248 |
| | Difference (%) | 23.1 | 36.7 | 24.8 |

indeed, the results were also similar, as the time-restricted modulation again performed much better than the original modulation. The results are presented in Tables 4 and 5 with the corresponding carbon assignments presented on Fig. 4. In this second test, we also used the sequence for quantitative purposes and determined the molar ratio of the two compounds. The results including comparison to ratio calculated from the measured weights during sample preparation are presented in Table 6.

Overall, the results are good and the maximum difference between minimum and maximum signals observed is comparable to the results obtained with quantitative $^{13}C$ measurements for all of the tested compounds, when using the time-restricted modulation scheme. While the errors for some signals are over 10%, they seem to be in the same direction and about the same magnitude for every spectra, suggesting that the errors are more systematic than random. Systematic errors do not affect relative comparison of samples, and can be corrected by measuring the pure compound in a similar environment and determining correction factors for each signal. Also, when using the sequence to determine the concentration ratio of compounds, the sequence seems to deliver results very close to quantitative $^{13}C$ with both modulations, when the average of multiple signals from the molecules are used (Table 6).

The results can also be compared with the calculated profile of the polarization transfer: in the worst measured case, the cholesterol, observed maximum signal differences are about 37% for original modulation and 25% for time-restricted modulation (Table 3), while the calculated differences for the polarization transfer itself are 3.6% and 12.7% for original and time-restricted modulation, respectively (Table 1). It is obvious that the original modulation scheme induces additional errors, but even for the time-restricted modulation, significant amount of the errors are probably caused by reasons other than the polarization transfer itself. This is supported by comparing the results for the time-restricted modulation and quantitative $^{13}C$: with maximum difference of 23%, quantitative $^{13}C$ experiment is only slightly better than the time-restricted

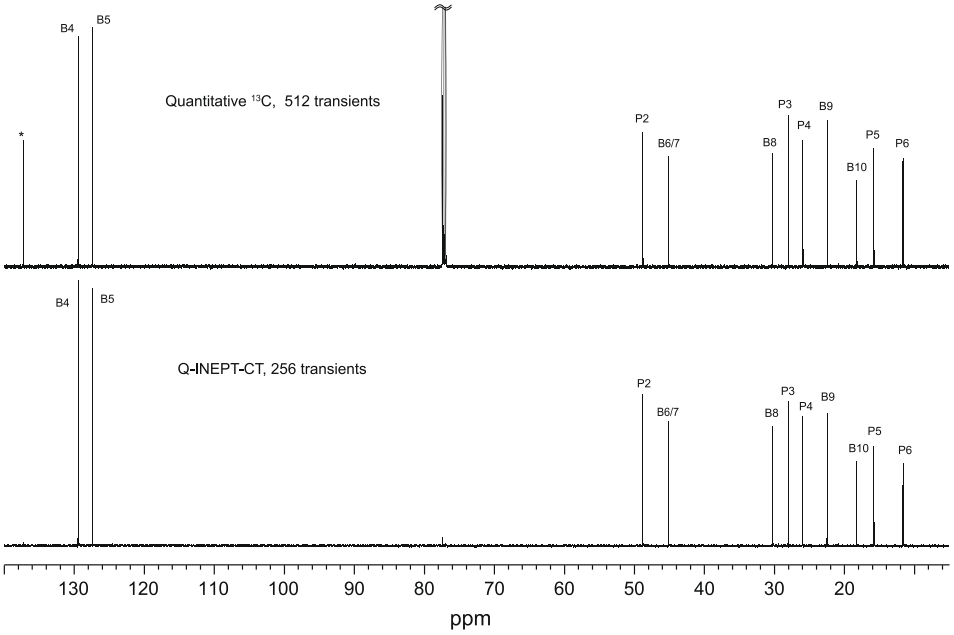


**Fig. 7.** A quantitative $^{13}$C spectrum compared to Q-INEPT-CT spectrum, obtained from sample #2 (ibuprofen and 3-methyl-2-pentanone). For quantitative $^{13}$C spectrum, only the region corresponding to the spectral width of Q-INEPT-CT is shown (quantitative $^{13}$C was actually recorded with larger spectral window to include the additional quaternary carbon signals). Quaternary carbon signals are marked by an asterisk in the quantitative $^{13}$C spectrum. The total measurement times were 8 h 34 min and 2 h 7 min for the quantitative $^{13}$C and Q-INEPT-CT spectra, respectively.

**Table 4**
The results for ibuprofen with both modulations and quantitative $^{13}$C. Quaternary carbons B1, B2 and B3 are not listed. The carbon assignments are given in Fig. 4.

| Carbon # | Chemical shift | $^{13}$C | Q-INEPT-CT | |
|---|---|---|---|---|
| | | | Original mod. | Time rest. mod. |
| B4 | 129.44 | 1.04 | 1.02 | 1.02 |
| B5 | 127.36 | 1.05 | 0.99 | 1.03 |
| B6 | 45.13 | 1.01 | 1.07 | 1.03 |
| B7 | 45.08 | 1.04 | 1.00 | 1.02 |
| B8 | 30.24 | 0.99 | 0.88 | 0.92 |
| B9 | 22.46 | 0.94 | 1.02 | 0.99 |
| B10 | 18.20 | 0.92 | 0.99 | 0.95 |
| | Min. integral | 0.918 | 0.879 | 0.923 |
| | Max. integral | 1.049 | 1.074 | 1.028 |
| | Difference | 0.131 | 0.195 | 0.105 |
| | Difference (%) | 13.1 | 19.5 | 10.5 |

**Table 5**
The results for 3-methyl-2-pentanone with both modulations and quantitative $^{13}$C. Quaternary carbon P1 is not listed. The carbon assignments are given in Fig. 4.

| Carbon # | Chemical shift | $^{13}$C | Q-INEPT-CT | |
|---|---|---|---|---|
| | | | Original mod. | Time rest. mod. |
| P2 | 48.77 | 1.02 | 0.99 | 1.02 |
| P3 | 28.05 | 1.04 | 1.14 | 1.08 |
| P4 | 25.92 | 1.05 | 0.88 | 0.97 |
| P5 | 15.76 | 0.96 | 1.03 | 1.00 |
| P6 | 11.63 | 0.93 | 0.96 | 0.93 |
| | Min. integral | 0.930 | 0.882 | 0.933 |
| | Max. integral | 1.051 | 1.138 | 1.078 |
| | Difference | 0.121 | 0.256 | 0.145 |
| | Difference (%) | 12.1 | 25.6 | 14.5 |

modulation Q-INEPT-CT with maximum signal difference of 25%. The good performance of the time-restricted modulation can be to some degree explained by looking at the theoretical response curve; while the overall difference between responses is larger, the main deviations from the relatively uniform response of $CH_3$ carbons exist on CH carbons with low $^1J_{CH}$ and on $CH_2$ carbons with high $^1J_{CH}$. However, both of these cases are relatively rare in organic molecules.

In addition to the residual errors arising from near-uniform polarization transfer, the offset performance of carbon pulses is crucial, as seen in Fig. 3. The offset effects (including any other experimental variation) seem to cause about 5% fluctuation, so adiabatic sweeps [15–17] or modern shaped inversion/refocusing pulses (such as PM-BEBOP [18]) can be used to further improve the performance of the sequence. For very high field instruments, even shaped 90° wideband carbon excitation pulse [18] could be used to extend the usable spectral width. These pulses can be quite easily substituted to the sequence, however care must be taken, at least in the case of long adiabatic sweeps, that the evolution of *J*-couplings is not affected or is accounted for.

Judging from the above results, the sequence works adequately for quantitative purposes as such, but there are still a few known factors which are not corrected. $T_2$ relaxation occurs during the execution of the pulse sequence, which can result significant signal loss for fast relaxing species. The homonuclear and long range heteronuclear couplings also evolve during the sequence, and while they are usually too small to make any significant impact, in some cases they might induce signal loss. In this sense, the time-restricted version of Q-INEPT-CT is superior to both normal Q-INEPT-CT and Q-DEPT/Q-DEPT$^+$, as its duration is significantly shorter. It should be also noted that all polarization transfer pulse sequences are longer and more complex than traditional quantitative $^{13}$C experiments, requiring more careful setup. However, due to their improved sensitivity, these polarization transfer sequences can be especially valuable when quantitative $^{13}$C data is required from relatively low concentrations and/or in short time.

## 4. Conclusions

The new Q-INEPT-CT experiment with the time-restricted modulation scheme can be used to obtain quantitative results compa-

**Table 6**
The molar ratio of ibuprofen to 3-methyl-2-pentanone in sample #2, calculated from NMR spectra and weight of the compounds during sample preparation. As the NMR results are so close to each other, the difference of NMR result to weighing is probably due impurities, moisture etc. The NMR results were calculated by integrating all signals from both molecules and calculating the average signal obtained per carbon, and determining the ratio of the two values.

| Pulse sequence/method | Molar ratio |
|---|---|
| Quantitative $^{13}C$ | 0.972 |
| Q-INEPT-CT, original mod. | 0.974 |
| Q-INEPT-CT, time-restricted mod. | 0.979 |
| By weight | 0.952 |

rable to standard quantitative $^{13}C$ spectroscopy, with greater sensitivity and/or in less time. The experiment is suitable for samples containing $^{1}J_{CH}$ values of about 115–170 Hz, which should cover most cases. In addition to the enhancement brought by polarization transfer, the necessary relaxation time is limited by proton $T_1$, which is usually an order of magnitude shorter than for carbon, yielding a much improved repetition rate and thus more signal in same amount of time.

Compared to Q-DEPT/Q-DEPT$^{+}$, Q-INEPT-CT offers shorter duration, utilizes constant-time approach (vide supra), does not rely on pulse length modulation and uses pulsed field gradients and composite pulses to achieve optimal performance. However, while it utilizes gradient pulses, they are only used for purging magnetization and can be substituted with a suitable phase cycle, meaning that the sequence can easily be implemented in older generation spectrometers as well.

## 5. Experimental

All experiments were conducted at 27.0 °C on a Varian $^{UNITY}$INOVA 600 MHz spectrometer using 5 mm triple resonance ($^{1}H$, $^{13}C$, $^{15}N$) gradient probehead. For pulse sequence evaluation, two samples containing a mixture of two compounds were used. Sample #1 contained ethylbenzene and cholesterol, and was chosen as it contained various types of carbon structures, while still retaining ethylbenzene originally used in the development of the Q-DEPT [4] sequence. The sample consisted of 27.0 mg of ethyl benzene mixed with 101.6 mg of cholesterol in ~0.7 ml $CDCl_3$. Sample #2 consisted of 70.2 mg of ibuprofen mixed with 35.8 mg of 3-methyl-2-pentanone in ~0.7 ml $CDCl_3$.

For sample #1, the longest $^{1}H$ $T_1$ relaxation time of ~20 s was determined for the aromatic protons of ethylbenzene. Therefore, in INEPT-CT experiments, the relaxation delay was set to 100 s, while the acquisition time was 2 s. For traditional quantitative $^{13}C$ spectra (inverse gated $^{1}H$ decoupling), 45° excitation pulse was used, with relaxation delay of 98 s and acquisition time of 2 s. The number of transients were 128 and 512 for Q-INEPT-CT and quantitative $^{13}C$ experiments, respectively. Spectral width was 25 kHz (165.7 ppm), while the transmitter carrier frequency was at 79.7 ppm. 90° pulse lengths were 14.1 and 5.4 μs for $^{13}C$ and $^{1}H$, respectively.

For sample #2, the longest $^{1}H$ $T_1$ relaxation time of ~5.5 s was determined for the P3 protons in 3-methyl-2-pentanone. For the INEPT-CT experiments, the relaxation delay was 27.5 s and the acquisition time was 2 s. For the quantitative $^{13}C$ spectrum, 45° excitation pulse was used, with relaxation delay of 58 s and acquisition time of 2 s. The number of transients were 256 and 512 for Q-INEPT-CT and quantitative $^{13}C$ experiments, respectively. Spectral width was 35.4 kHz (234.8 ppm) for quantitative $^{13}C$ and 22.7 kHz (150.7 ppm) for Q-INEPT-CT, while the transmitter carrier frequency was at 110.7 ppm for quantitative $^{13}C$ and 76.8 ppm for Q-INEPT-CT. 90° pulse lengths were 13.9 and 5.0 μs for $^{13}C$ and $^{1}H$, respectively.

In Q-INEPT-CT spectra, the PFG durations were 4 ms (G1) and 200 μs (G2 and G3), while the PFG strengths were 53.2 G/cm (G1 and G2) and 62.1 G/cm (G3). Eddy current recovery delay was 150 μs. WALTZ-16 $^{1}H$ decoupling scheme was used during acquisition [19]. All FIDs were apodized using an exponential function (0.5 Hz line broadening) prior to Fourier transform. Data was analyzed with a custom analysis program written in Java (ImatraNMR), which is designed to speed up the integration of the multiple regions from multiple spectra. The integration ranges for each signal were between 0.06–0.2 ppm, depending on linewidth and possible signal overlap. The program along with source code is available for non-commercial and academic uses upon request from the author.

## Acknowledgments

The author, A.V. Mäkelä gratefully acknowledges financial support from the Finnish Funding Agency for Technology and Innovation (Tekes).

## Appendix A. Supplementary data

Supplementary data associated with this article can be found, in the online version, at doi:10.1016/j.jmr.2010.02.015.

## References

[1] Ŝárka Mierisová, M. Ala-Korpela, MR spectroscopy quantitation: a review of frequency domain methods, NMR Biomed. 14 (2001) 247–259.
[2] D.M. Doddrell, D.T. Pegg, Assignment of proton-decoupled $^{13}C$ spectra of complex molecules by using polarization transfer spectroscopy. A superior method to off-resonance decoupling, J. Am. Chem. Soc. 102 (1980) 6388–6390.
[3] D.M. Doddrell, D. Pegg, M. Bendall, Distortionless enhancement of NMR signals by polarization transfer, J. Magn. Reson. 48 (1982) 323–327.
[4] T.J. Henderson, Sensitivity-enchanced quantitative $^{13}C$ NMR spectroscopy via cancellation of $^{1}J_{CH}$ dependence in DEPT polarization transfers, J. Am. Chem. Soc. 126 (2004) 3682–3683.
[5] B. Jiang, N. Xiao, H. Liu, Z. Zhou, X. an Mao, M. Liu, Optimized quantitative DEPT and quantitative POMMIE experiments for $^{13}C$ NMR, Anal. Chem. 80 (2008) 8293–8298.
[6] S. Heikkinen, M.M. Toikka, P.T. Karhunen, I.A. Kilpeläinen, Quantitative 2D HSQC (Q-HSQC) via suppression of *J*-dependence of polarization transfer in NMR spectroscopy: application to wood lignin, J. Am. Chem. Soc. 125 (2003) 4362–4367.
[7] H. Koskela, I. Kilpeläinen, S. Heikkinen, Some aspects of quantitative 2D NMR, J. Magn. Reson. 174 (2005) 237–244.
[8] O. Sørensen, G. Eich, M. Levitt, G. Bodenhausen, R. Ernst, Product operator formalism for the description of NMR pulse experiments, Prog. Nuclear Magn. Reson. Spectr. 16 (1984) 163–192.
[9] D.P. Burum, R.R. Ernst, Net polarization transfer via a *J*-ordered state for signal enhancement of low-sensitivity nuclei, J. Magn. Reson 39 (1980) 163–168.
[10] R.R. Ernst, G. Bodenhausen, A. Wokaun, Principles of Nuclear Magnetic Resonance in One and Two Dimensions, 2nd ed., Oxford University Press, Oxford, UK, 1992.
[11] L. Lasdon, A. Warren, A. Jain, M. Ratner, Design and testing of a generalized reduced gradient code for nonlinear programming, ACM Trans. Math. Softw. 4 (1978) 34–50.
[12] A.J. Shaka, Composite pulses for ultra-broadband spin inversion, Chem. Phys. Lett. 120 (1985) 201–205.
[13] A.J. Shaka, P.B. Barker, R. Freeman, Experimental demonstration of wideband spin inversion, J. Magn. Reson. 67 (1986) 580–584.
[14] G. Vuister, F. Delaglio, A. Bax, The use of $^{1}J_{C\alpha H\alpha}$ coupling constants as a probe for protein backbone conformation, J. Biomol. NMR 3 (1993) 67–80.
[15] T. Hwang, P.C.M. van Zijl, M. Garwood, Fast broadband inversion by adiabatic pulses, J. Magn. Reson. 133 (1998) 200–203.
[16] M. Garwood, L. DelaBarre, The return of the frequency sweep: designing adiabatic pulses for contemporary NMR, J. Magn. Reson. 153 (2001) 155–177.
[17] M.A. Smith, H. Hu, A.J. Shaka, Improved broadband inversion performance for NMR in liquids, J. Magn. Reson. 151 (2001) 269–283.
[18] T.E. Skinner, K. Kobzar, B. Luy, M.R. Bendall, W. Bermel, N. Khaneja, S.J. Glaser, Optimal control design of constant amplitude phase-modulated pulses: application to calibration-free broadband excitation, J. Magn. Reson. 179 (2006) 241–249.
[19] A.J. Shaka, J. Keeler, T. Frenkiel, R. Freeman, An improved sequence for broadband decoupling: WALTZ-16, J. Magn. Reson. 52 (1983) 335.